Chiral-odd GPDs

Towards improved hadron femtography with hard exclusive reactions, edition IV, JLab, 2025

Jun-Young Kim

In collaboration with C. Weiss

Chiral-odd GPDs: Non-perturbative structure

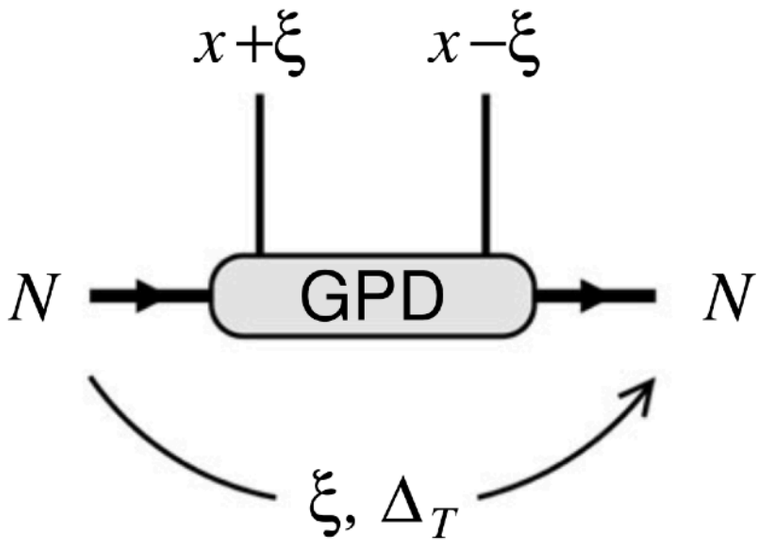

[S. Diehl et al., EPJA (2025)]

$$\mathscr{M}[i\sigma^{+j}] = \int \frac{dz^-}{2\pi} e^{iP^+z^-x} \langle N(p',s') \,|\, O^j_{\rm QCD}(z) \,|\, N(p,s)\rangle \,|_{z^-=\mathbf{z}_\perp=\mathbf{0}}$$

$$= \sum_{F=H_T,\tilde{H}_T,E_T,\tilde{E}_T} \mathscr{K}^j_F(\Delta,P,n;s',s) F(x,\xi,t)$$

$$O^j_{\rm QCD}(z) = \bar{\psi}(-z/2)[-z/2,z/2] i\sigma^{+j} \psi(z/2)$$

Based on [JYKim, C.Weiss, PRD (2025)]
[JYKim, C.Weiss, In preparation]

Multipole expansion

Systematic / Mechanical interpretation

Large-N_c analysis

Multipole GPDs at large N_c

Large-N_c relation

Chiral dynamics

Chiral quark-soliton model

Polynomiality and sum rules

Dynamical/kinematical hierarchies

Numerical results

Chiral-odd GPDs

Comparison with the lattice QCD

Multipole expansion

Symmetric/Colinear frame

$$\Delta_T \neq 0,\ P_T = 0 \qquad P\cdot n = 1, \quad t = \Delta^2, \quad \xi = -\frac{\Delta\cdot n}{2P\cdot n}$$

Two vectors : Polarization operator (σ_T)

Momentum transfer (Δ_T)

QCD operator		Polarization operator		Orbital angular momentum	
$\mathscr{M}[\gamma^+, \gamma^+\gamma^5]$		$\mathbf{1}, \sigma^{\mathbf{3}}$		$X_0 = 1$	$(L_z = 0)$
$\mathscr{M}[\sigma^{+j}]$	$=$	σ_T^i	$\otimes$	$X_1^i = \frac{\Delta^i}{\lvert\mathbf{\Delta_T}\rvert}$	$(L_z = \pm 1)$
				$X_2^{ij} = \frac{\Delta^i\Delta^j}{\lvert\mathbf{\Delta_T}\rvert^2} - \frac{1}{2}\delta^{ij}$	$(L_z = 0, \pm 1, \pm 2)$

$$\mathscr{M}[\sigma^{+j}] \propto i\epsilon^{3jm}\sigma^m X_0 G_0 + X_1^j \frac{\lvert\mathbf{\Delta_T}\rvert}{2M_N} G_1 + i\epsilon^{3jm}\sigma^3 X_1^m \frac{\lvert\mathbf{\Delta_T}\rvert}{2M_N}\tilde{G}_1 + i\epsilon^{3jl}\sigma^m X_2^{mj}\frac{\lvert\mathbf{\Delta_T}\rvert^2}{4M_N^2} G_2$$

$$G_0 = (1-\xi^2)H_T + \frac{\lvert\Delta_T\rvert^2}{2M_N^2}\tilde{H}_T - \xi^2 E_T + \xi\tilde{E}_T \qquad \tilde{G}_1 = \tilde{E}_T - \xi E_T$$

$$G_1 = 2\tilde{H}_T + E_T - \xi\tilde{E}_T \qquad G_2 = -2\tilde{H}_T$$

[JYKim, C.Weiss, PRD (2025)]

Angular momentum selection rule

Parity and time-reversal symmetries

Emergence of the quadrupole structure

Large-N_c analysis

Multipole GPDs at large N_c

Multipole GPDs are now homogeneous in N_c.

They become kinematically enhanced with increasing multipole order in the large-N_c limit.

$$G_{\mathrm{mf},n} \propto M_N^n N_c \times \text{function}(N_c x, N_c \xi, t)$$

$$M_N = O(N_c^1)$$

$$O(N_c^2) = G_{\mathrm{mf},0} = H_T^{u-d} + \left(\frac{t}{8M_N^2} - \frac{\xi^2}{2} \right) E_T^{u-d} + \xi \tilde{E}_T^{u-d}$$

$$O(N_c^3) = \tilde{G}_{\mathrm{mf},1} = \tilde{E}_T^{u-d} - \xi E_T^{u-d}$$

$$O(N_c^3) = G_{\mathrm{mf},1} = 2\tilde{H}_T^{u+d} + E_T^{u+d} \equiv \bar{E}_T^{u+d}$$

$$O(N_c^4) = G_{\mathrm{mf},2} = E_T^{u-d}$$

[JYKim, C.Weiss, PRD (2025)]

[JYKim, 2506.21013]

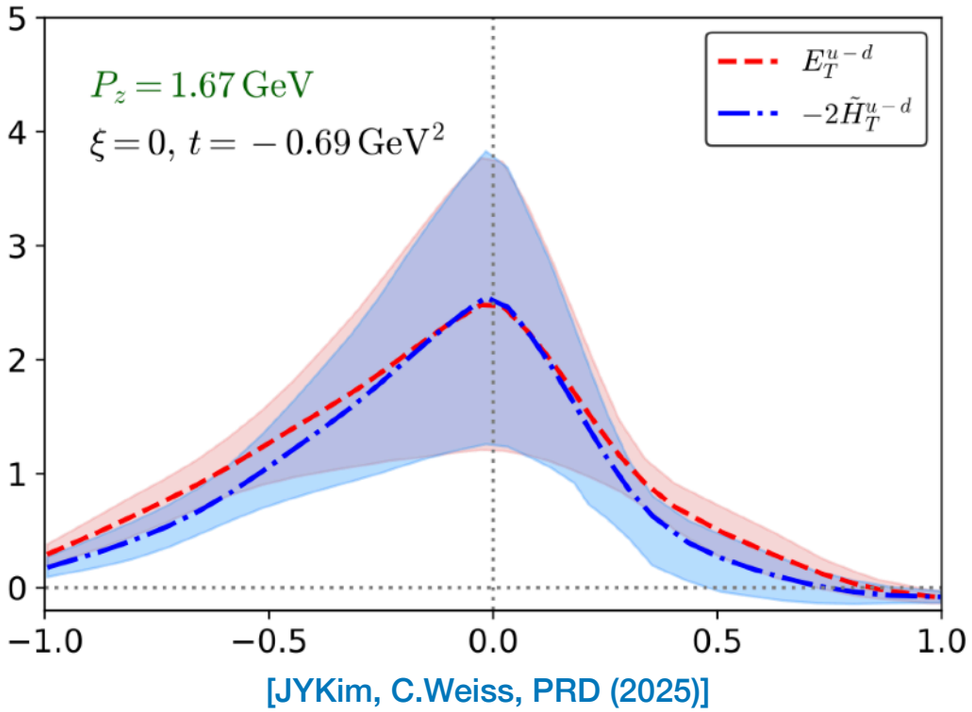

[JYKim, C.Weiss, PRD (2025)]

[P. Schweitzer, C.Weiss, PRC (2016)]

Large-N_c relation

In the strict large-N_c limit, the relation between the two quadrupole GPDs is given as follows:

$$E_T^{u-d} = -2\tilde{H}_T^{u-d}$$

Test of the large-N_c relation: LQCD data show good agreement with the large-N_c prediction.

[C. Alexandrou et al., PRD (2022)]

[K. Tezgin et al., PRD (2024)]

Chiral quark-soliton model

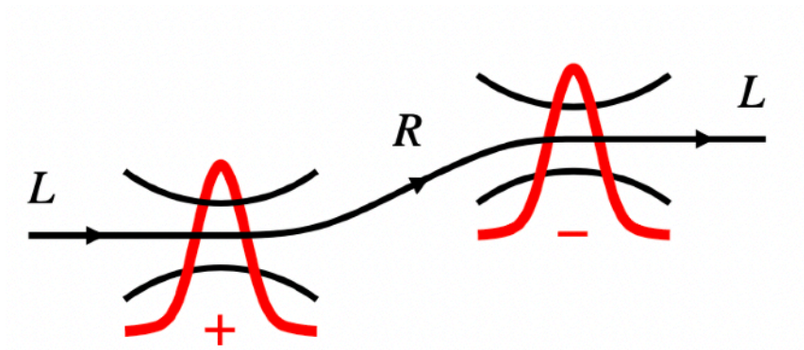

Effective chiral theory in the large-N_c limit of QCD

Embodies low-energy effective theory

Derived from QCD instanton vacuum

Mechanism of the chiral symmetry breaking

Degrees of freedom→Goldstone boson + Massive quark

Effective action

$$S = -\int d^4x \bar{\psi}[i\partial^\mu\gamma_\mu + iMU^{\gamma_5}]\psi$$

Semicalssical approximation (mean-field picture)

$$\left.\frac{\delta S[U]}{\delta U}\right|_{U=U_{\rm cl}} = 0$$

[D. Diakonov, V. Petrov P. Pobylitsa, NPB (1988)]
[Ch. Christov et al., PPNP (1996)]

Effective operator

The QCD operator is matched to the effective degrees of freedom.

It is obtained with parametrically the same accuracy as the effective action.

$$O^j_{\rm QCD}(z) = \bar{\psi}(-z/2)[-z/2,z/2]i\sigma^{+j}\psi(z/2)$$

↓

$$O^j_{\rm eff}(z) = \bar{\psi}(-z/2)i\sigma^{+j}\psi(z/2)$$

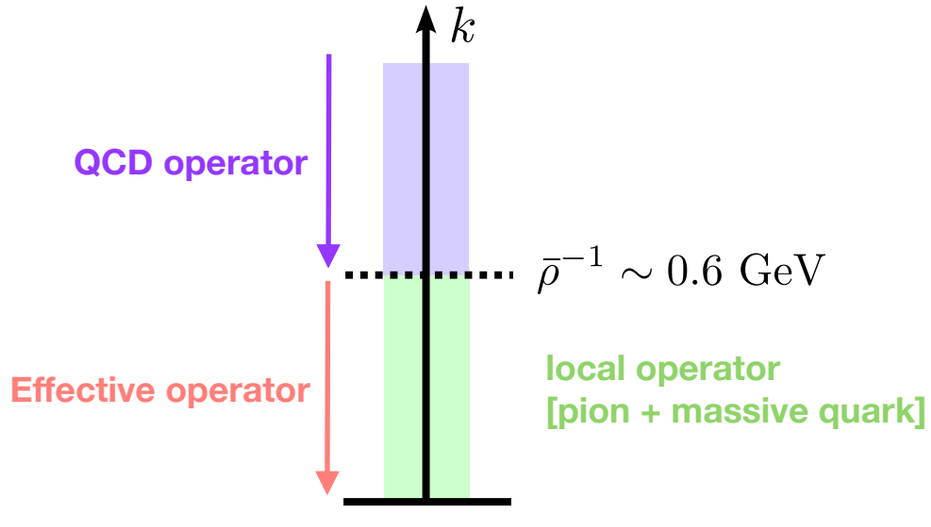

[D. Diakonov, M. Polyakov, C.Weiss., NPB (1997)]
[J. Balla, M. Polyakov, C.Weiss., NPB (1998)]

Mean-field GPDs: Polynomilaity and sum rules

Matrix element of the effective operator

$$\langle N' | O^j_{\rm eff}(z) | N \rangle = \lim_{T\to\infty} \frac{1}{Z} \mathcal{N} e^{ip_4 \frac{T}{2} - ip'_4 \frac{T}{2}} \int d^3x \int d^3y e^{-i\mathbf{p}'\cdot\mathbf{y} + i\mathbf{p}'\cdot\mathbf{x}}$$
$$\int D\psi D\psi^\dagger DU J_{N'}(\mathbf{y}, T/2) O^j_{\rm eff}(z) J_N(\mathbf{x}, -T/2) \exp[-S]$$

Three point correlation function
→ semiclassical approximation

$$G_{\rm mf} = \sum_n \langle n | \ldots | n \rangle$$

Multipole GPDs in the single particle representation

General constraints on GPDs [JYKim, C.Weiss, PRD (2025)] [P. Schweitzer et al, PRD (2002)] [P. Schweitzer et al, PRD (2003)]

$$\int dx\, x^{m-1} G_{\rm mf,0}(x,\xi,t) = \sum_{i={\rm even}}^{m+1} \xi^i F^{i,m-1}_{\rm mf,0}(t)$$

Polynomilaity: Discrete symmetry (parity, time-reversal) and Minimal generalization of the rotation symmetry (hedgehog symmetry)

$$\int dx\, G_{\rm mf,0}(x,\xi,t) = H^{u-d}_T(t) + \left(\frac{t}{8M_N^2} - \frac{\xi^2}{2} \right) E^{u-d}_T(t)$$

Sum rules: Hedgehog symmetry and selection rules for quantum numbers of the single particle wave function

Enhances the reliability of predictions based on the mean-field picture.

Mean-field GPDs: Dynamical/kinematical hierarchies

Organizing the GPDs in multipole order

Kinematical enhancement: Due to the parametric enhancement in the N_c scaling of multipole GPDs, their magnitudes increase at non-exceptional x as the multipole order rises.

Dynamical (chiral) enhancement: Due to the additional r-weight, long-range contributions are amplified as the multipole order increases, leading to an enhancement at small x in PDFs.

$$G_{\mathrm{mf},n} \propto M_N^n N_c \int d^3r\, r^n \rho_n(r) \quad \text{[moment of n-pole GPD]}$$

$$M_N = O(N_c^1)$$

$\rho(r)$ [dimensionless dist.]

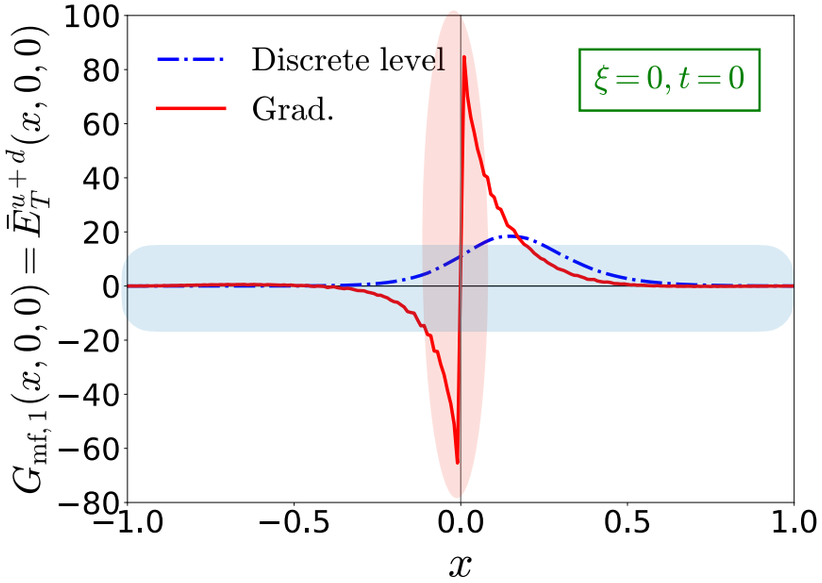

Multipole structure	$G_{\mathrm{mf},0}$ (mo.)		$G_{\mathrm{mf},1}$ (di.)		$\tilde{G}_{\mathrm{mf},1}$ (di.)		$G_{\mathrm{mf},2}$ (Quad.)
N_c scaling	N_c^2	$<$	N_c^3	$\sim$	N_c^3	$<$	N_c^4
Kinematical hierarchy	H_T^{u-d}	$<$	$2\tilde{H}_T^{u+d} + E_T^{u+d}$	$\sim$	$\tilde{E}_T^{u-d}$	$<$	E_T^{u-d}
Dynamical hierarchy	H_T^{u-d}	$<$	$2\tilde{H}_T^{u+d} + E_T^{u+d}$	$\sim$	$\tilde{E}_T^{u-d}$	$<$	E_T^{u-d}

Chiral-odd GPDs: Monopole

Discrete level ~ Valence quark contribution

Gradient expansion (Grad.) ~ Dirac-sea quark contribution

Captures long-distance contribution or chiral dynamics.

Forward limit

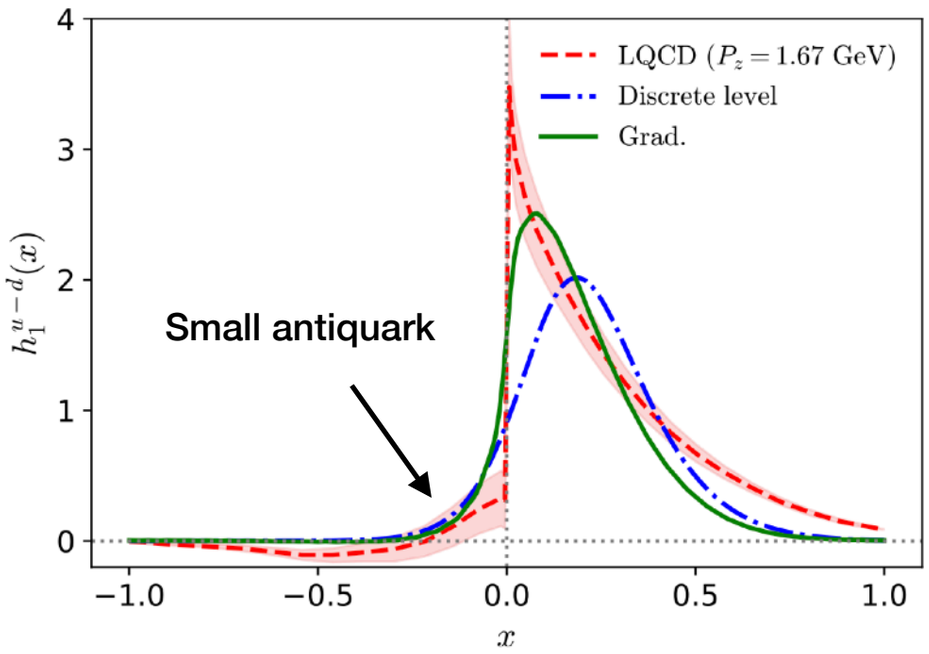

$$g_T^{u-d} = 0.85\,{}^{(0.76)}_{(0.09)}\ [\text{lev}] \quad = 0.88\,{}^{(0.80)}_{(0.08)}\ [\text{grad}]$$

quark

antiquark

$g_T^{u-d} = 0.97\ (5)$ [LQCD] [S. Park et al., PRD (2022)]

Monopole GPD H_T^{u-d}

Valence quark approximation is comparable to the gradient expansion.

Antiquark (quark) contributions are very small (large).

Both results show good agreement with lattice QCD.

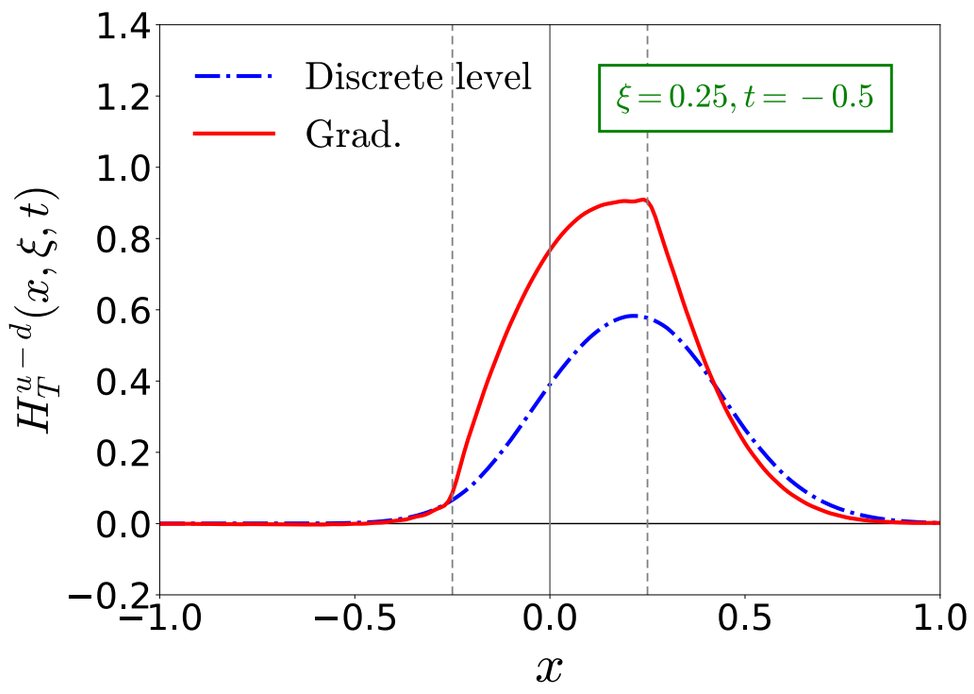

Chiral-odd GPDs: Dipole

Forward limit

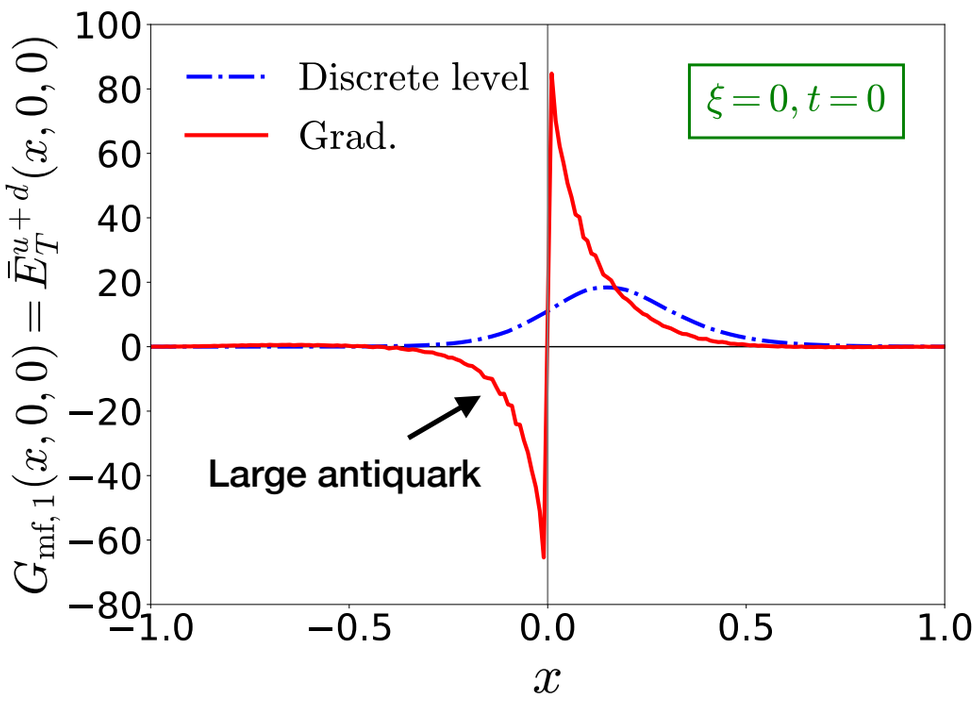

ξ-even dipole GPD $\bar{E}_T^{u+d} = 2\tilde{H}_T^{u+d} + E_T^{u+d}$

The shape of the GPD in the valence quark approximation differs from that in the gradient expansion.

Quark and antiquark contributions become large for Grad.

Strong antisymmetric behavior: sea quark contribution cancels in the first moment → quark model prediction remains valid.

$$\kappa_T^{u+d} = 7.56\,{}^{(6.36)}_{(1.20)} \quad [\mathrm{lev}] \quad = 4.25\,{}^{(9.37)}_{(-5.12)}\ [\mathrm{grad}]$$

Second moment reveals significant dominance of sea quarks.

ξ-odd dipole GPD $\tilde{E}_T^{u-d}$

Antisymmetric in ξ → first moment vanishes.

$$\int dx\, \tilde{E}_T^{u-d}(x, \xi = 0.25, t = -0.5\ \mathrm{GeV}^2) = 0$$

A nodal point appears.

The predicted shape of the GPD strongly depends on the underlying dynamics.

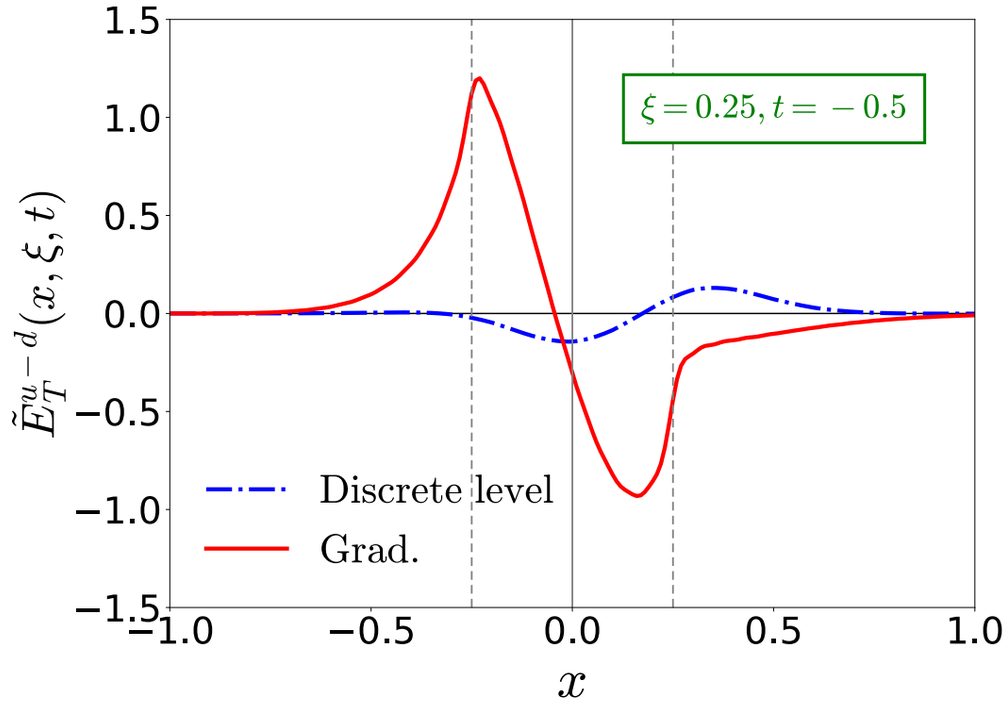

Chiral-odd GPDs: Quadrupole

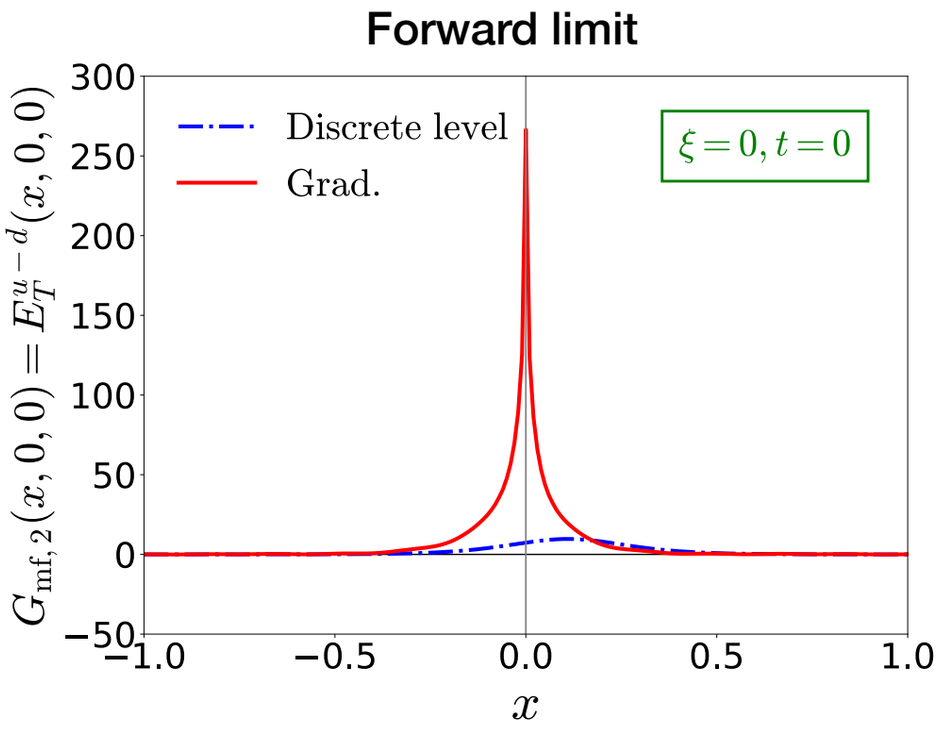

Quadrupole GPD $E_T^{u-d} = -2\tilde{H}_T^{u-d}$

A very strong chiral enhancement is predicted.

The distribution is nearly symmetric, resulting in a large first moment.

$$Q_T^{u-d} = 3.95\,{}^{(2.92)}_{(1.03)} \quad [\mathrm{lev}] \quad = 17.38\,{}^{(8.29)}_{(9.09)} \quad [\mathrm{grad}]$$

The quadrupole structure is clearly distinguished from monopole and dipole ones by its antiquark dominance.

Comparison with LQCD

Lattice QCD also predicts antiquark dominance.

This dominance cannot be explained by the valence quark approximation.

$$\int dx\, E_T^{u-d}(x,0,t = -0.69\ \mathrm{GeV}^2)$$

$$= 0.74 \quad [\mathrm{lev}] \quad = 2.62 \quad [\mathrm{grad}]$$

$$= 2.10\ (67) \quad [\mathrm{LQCD}]$$

[C. Alexandrou et al., PRD (2022)]

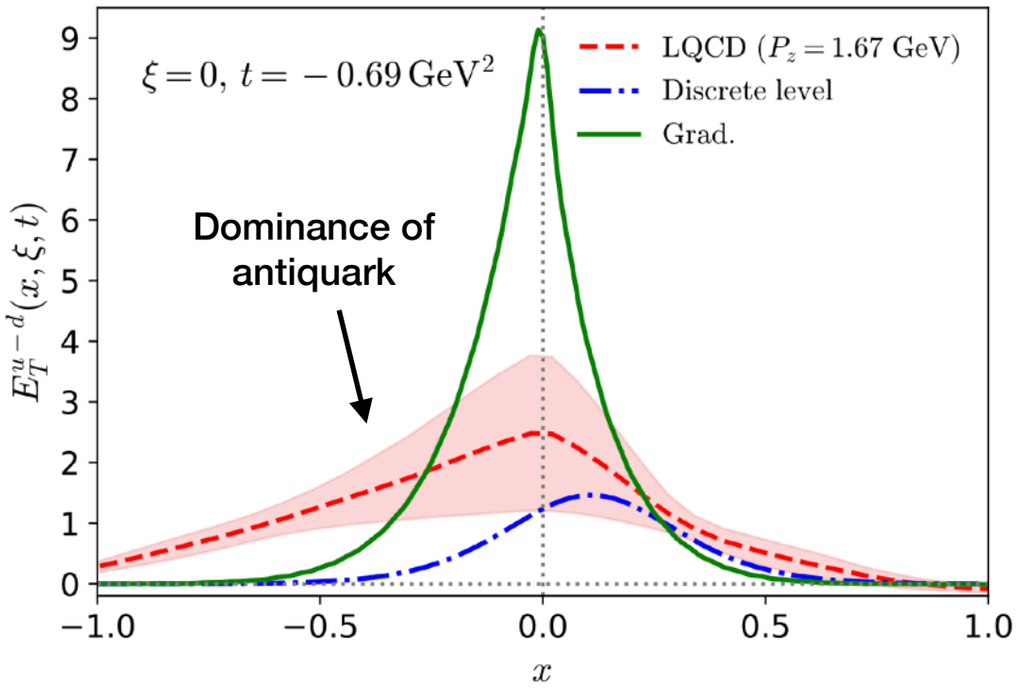

Summary

Conclusions

Multipole expansion provides a systematic classification of GPDs from the perspective of non-perturbative (chiral) physics.

General constraints on GPDs, such as polynomiality and sum rules, are satisfied within the mean-field picture.

Kinematical and dynamical hierarchies among GPDs have been established.

Chiral dynamics play an increasingly important role with higher multipole orders, leading to enhancements at small x.

This study will provide guidance for parameterizing the GPDs.

Outlook

The same multipole analysis can be applied to chiral-even GPDs (vector and axial-vector).

This approach can also be extended to GPDs involving higher-spin particles and their transitions, revealing an even richer multipole structure.

Thank you very much!

Chiral-odd GPDs: First moment

Tensor form factors [N.Y.Ghim et al., PRD (2025)]

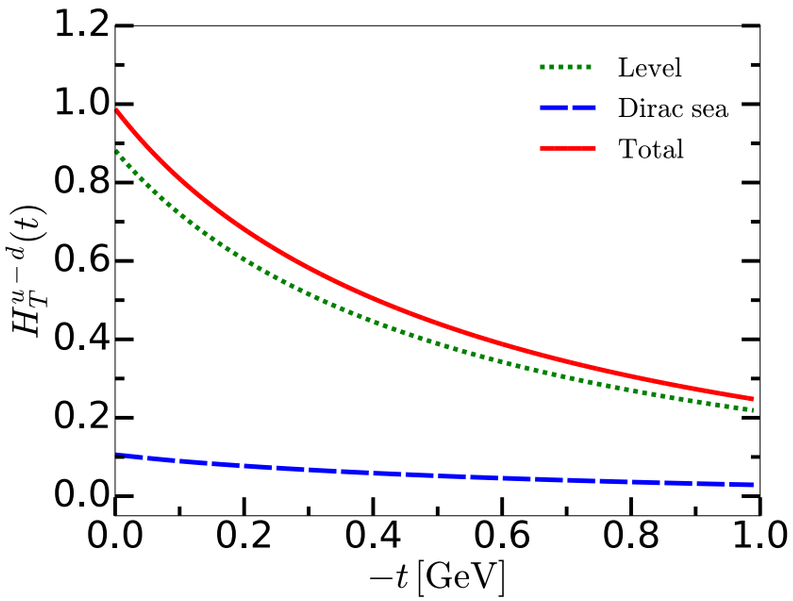

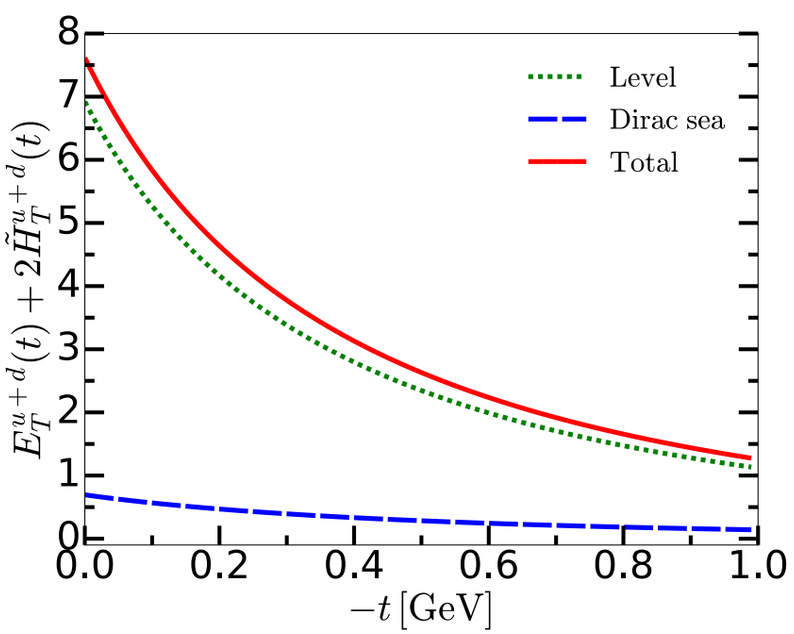

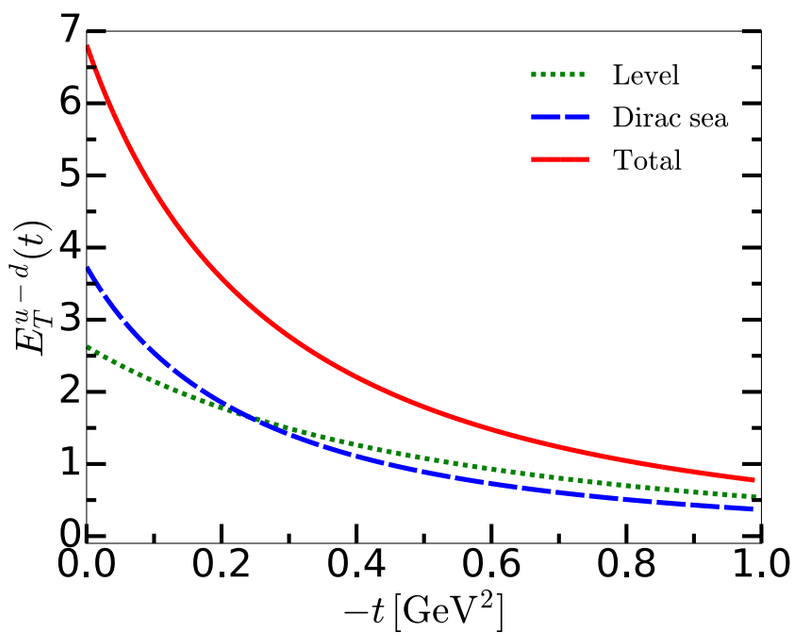

Pion mass dependence

[N.Y.Ghim et al., PRD (2025)]